

^{1,2} Yuzhuo Wang
^{2,3,*} Zhichao Xu
⁴ Yunshan Chen
¹ Kai Li

Application of computer technology to numerical simulation of hydrothermal variation of subgrade enhanced by seepage drainage geograge under freeze-thaw cycle



Abstract: - In seasonal frozen soil areas, engineering problems are common due to the high water content of subgrade soil. In view of this phenomenon, a new type of percolating drainage geogrid (SDG) is proposed for cooling and drainage. The changes of soil temperature and moisture at different time points were analyzed through computer simulation laboratory model test, and the changes and distribution of soil temperature and moisture under freeze-thaw conditions were obtained. The temperature and moisture changes and their distribution obtained by computer modeling agree with the experimental results. By optimizing the soil materials of the model samples, the changes of temperature and moisture with time under freeze-thaw conditions were more significant. Therefore, it can be inferred that, without changing the configuration of the percolation drain grid, the cooling drainage performance of the percolation drain grid can be improved under the same conditions by changing the heat transfer coefficient or the macroporous filling material. It provides theoretical support and data guarantee for the reinforcement of subgrade percolation and drainage grid in cold area.

Keywords: Seasonal frozen soil; Seepage geogrid; Calculation model; Numerical simulation; Cooling drainage.

I. INTRODUCTION

The subgrade is the foundation of the whole road structure, and its stability directly affects the function and use of the road structure. The subgrade can only maintain the cohesiveness of the subgrade soil particles within a certain moisture content range to ensure that the pavement does not deform and damage [1-4]. The high water content of subgrade will seriously affect its stability and service life, especially wet and over-wet soil subgrade, which are affected by factors such as surface water (rain and snow melting, etc.), groundwater[5-8]. It has a great influence on the stability and durability of the pavement structure [9-12].

In view of the problem of excessive moisture content of subgrade soil in seasonal frozen soil areas, the author used a new type of SDG developed by the Cold Region Science and Engineering Research Institute of Northeast Forestry University.

II. NUMERICAL SIMULATION ANALYSIS

A. Introduction of numerical simulation technology

As early as the 1960s, American scholar Kraft applied finite element to the stability analysis of earth-rock dams. In the past half century, in the field of geotechnical engineering, numerical simulation has been greatly developed and a lot of complicated engineering problems were well solved by this kind of technology. Also, with the development of computers, more complex large-scale model tests and some geotechnical problems which are too resource-intensive and difficult to make into solid models can be solved in this way. Computer's appearance and development not only saves a lot of valuable time and resources, but also provides a large room for numerical simulation's development.

Numerical simulation has many advantages applying to the experimental research of geotechnical engineering, especially for the soil's indoor model test under freezing and thawing cycles, the whole test time can be greatly shortened, and the test conditions which are difficult to apply in the room can be solved at the same time. Also, different kinds of test conditions can be repeated multiple times, the temperature and moisture changes can be found and the results and assignment conditions of the calculation model can be verified in a short time.

¹ College of Agriculture and Water Conservancy Engineering, Sui Hua University, Suihua, 152061, China

² Field Scientific Observation and Research Station of the Ministry of Education-Geological Environment System of Permafrost Area in Northeast China, Northeast Forestry University, Harbin 150040, China

³ National Demonstration Center for Experimental Civil Engineering Education, Hunan City University, Yiyang 413002, China

⁴ Key Technology Laboratory of Digital Urban Rural Spatial Planning in Hunan Province, Hunan City University, Yiyang 413002, China

*Corresponding author: Zhichao Xu

Copyright © JES 2024 on-line : journal.esrgroups.org

B. Establishment of SDG model

Since the cross section of the grid tube is circular, the meshing density of the soil around the circular tube is very large and the number is large. In order not to affect the calculation parameters of the model and simplify the calculation, also mechanical factors are not considered in this experiment, the cross section of the grid tube is changed to rectangle, but the contact area of the grid tube and the soil still maintains, which causes a 20% reduction in the model's volume. Comparing the results between indoor model test and numerical simulation, it is found that the volume change of the SDG has little effect on the soil temperature and water content. The mesh of the seepage drainage grid is divided into tetrahedral units, and the total number of divided domain units is 66,113.

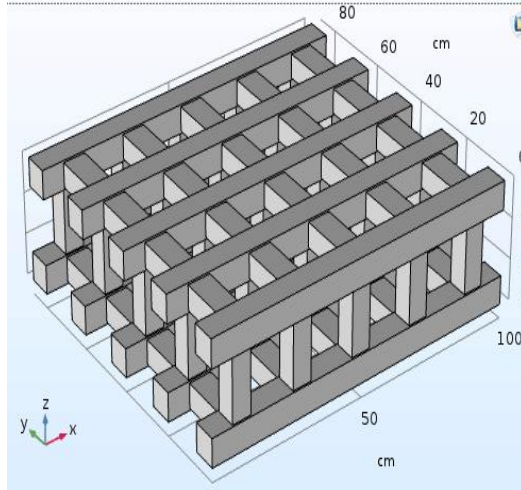


Fig.1 The graph of equivalent grating

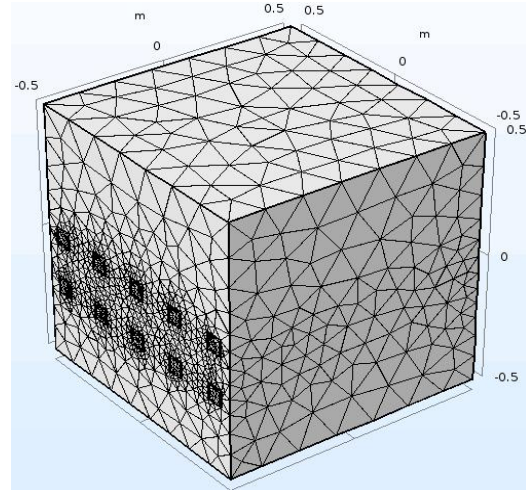


Fig.2 Model soil mesh division

C. Selection of parameters

For the simulation of moisture and heat transfer, some parameters (such as thermal conductivity and specific heat capacity) are indispensable. These parameters have been obtained through previous laboratory tests, as shown in the table 1.

Tab.1 The thermal parameter of the soilsamples

ρ_d (kg/m^3)	W (%)	C_u $\text{kJ}/(\text{m}^3 \cdot \text{K})$	C_f $\text{kJ}/(\text{m}^3 \cdot \text{K})$	λ_u $[\text{W}/(\text{m} \cdot \text{K})]$	λ_f $[\text{W}/(\text{m} \cdot \text{K})]$	α_u $(\times 10^3 \text{m}^2/\text{h})$	α_f $(\times 10^3 \text{m}^2/\text{h})$
1581	23	2843.8	2459.1	1.26	1.59	1.59	2.49
1600	25	3011.0	2375.4	1.28	1.80	1.52	2.73

Freezing point ($^{\circ}\text{C}$)	Melting point ($^{\circ}\text{C}$)	Water conductivity (m/s)	Water density (kg/m^3)	Ice density (kg/m^3)	Latent heat (kJ/kg)	Initial moisture content (m^3/m^3)
-3	0.5	6.5×10^{-8}	1000	900	334.7	0.3

D. Selection of controlling equation

Solving the multiphysics coupling is essentially the solution of partial differential equations, since COMSOL Multiphysics has many embedded controlling equations in water and heat transfer module, it is important to select the governing equation according to the actual conditions.

1) controlling equation of heat transfer

In order to solve the soil temperature field, it is necessary to establish a differential equation that can describe the heat conduction problem which must be based on Fourier's law and the law of conservation of energy. For the purpose of simplifying this problem, it is assumed that the soil is homogeneous and isotropic, and its thermal conductivity λ , specific heat C_d and density ρ are treated as constants. When there is no heat flow distribution in the soil, the Fourier governing equation can be reduced to the following form:

$$\frac{\partial \theta}{\partial t} = \frac{\lambda}{C_p} \left(\frac{\partial^2 \theta}{\partial x^2} + \frac{\partial^2 \theta}{\partial y^2} + \frac{\partial^2 \theta}{\partial z^2} \right)$$

The description of the heat transfer in soil must also list the conditions that meet the specific conditions of the test: initial conditions - indicating the temperature distribution of the soil at the beginning of the process; boundary conditions - the mutual heat exchange between the soil and the surrounding medium at the geometric boundary effect. The initial conditions and boundary conditions are collectively referred to boundary conditions. The complete mathematical description of any specific heat transfer problem should include the thermal differential equation and the boundary condition. For the problem of stable heat transfer, the initial conditions are meaningless. In this test, the process of temperature rising is an unsteady transfer problem, and when the temperature lowers, the heat transfer problem is stabilized, but the temperature rises and falls in the grid is unsteady, therefore, solving this problem of unsteady temperature conduction is most suitable.

2) *controlling equation of water migration*

There are two kinds of seepage modes for water migration in soil, stable seepage and unsteady seepage. Stable seepage: The unfrozen water migrates in frozen soil under constant temperature gradient, the migration amount does not change with time, and it belongs to stable seepage. Unsteady seepage: Under the condition of the freezing front and the temperature gradient change in the frozen soil, the migration amount changes with time, which is an unsteady seepage condition. According to the temperature change and distribution of indoor test, water migration belongs to unsteady seepage, which needs to be solved by hydro-thermal coupling equation. Harlan model and Taylor model are commonly used.

Harlan Model:

$$\frac{\partial}{\partial x} \left(\lambda \frac{\partial \theta}{\partial x} \right) = c \rho \frac{\partial \theta}{\partial t} - L \frac{\partial W_i}{\partial t}$$

Water flow equation:

$$\frac{\partial}{\partial x} \left(K \frac{\partial \varphi}{\partial x} \right) = \frac{\partial W_w}{\partial t} + \frac{\rho_i}{\rho_w} \frac{\partial W_i}{\partial t}$$

$$\left(c \rho + L \frac{\partial W_w}{\partial T} \right) \frac{\partial \theta}{\partial t} = \frac{\partial}{\partial x} \left(\lambda \frac{\partial \theta}{\partial x} \right) + L \left(K \frac{\partial \varphi}{\partial x} \right)$$

Taylor and Luthin Model:

$$\frac{\partial}{\partial x} \left(D \frac{\partial W_w}{\partial x} \right) = \frac{\partial W_w}{\partial t} + \frac{\rho_i}{\rho_w} \frac{\partial W_i}{\partial t}$$

Where: λ is the thermal conductivity; c is the specific heat; ρ is the density; L is the latent heat of melting of ice; θ is the temperature; x is the coordinate; t is the time; W_i is the ice content; W_w is the volumetric water content; K is The coefficient of moisture conductivity; φ is the soil water potential; D is the water diffusion coefficient.

For the flux of unfrozen water in frozen soil, using Darcy's law for unsaturated soil motion:

$$Q = -D_w(\theta)W_u$$

The water movement in frozen soil and unfrozen soil can be described by a consistent equation, which is convenient for unified calculation.

For frozen soil and unfrozen soil, the main role of water is the phase of water. Therefore, the changes in density, thermal conductivity, volumetric heat capacity, temperature and water content before and after the water phase change are known. When the properties of the frozen soil are uniform and the temperature is constant:

$$\rho C_{pi} \cdot \nabla T + \nabla \cdot \mathbf{q} = Q + Q_p + Q_{vd}$$

Where:

$$\mathbf{q} = -\lambda \nabla T$$

$$\rho = \theta \rho_u + (1 - \theta) \rho_f$$

$$C_p = \frac{1}{\rho} (\theta_u \rho_u C_{pu} + (1 - \theta) \rho_f C_{pf}) + L \frac{\partial \theta}{\partial T}$$

$$\lambda = \theta \lambda_{i1} + (1 - \theta) \lambda_f$$

$$\frac{\partial \alpha_m}{\partial T} = \frac{1}{2} \cdot \frac{(1 - \theta) \rho_f - \theta \rho_{i1}}{\theta \rho_{i1} + (1 - \theta) \rho_f}$$

When temperature changes with time:

$$\rho C_p \frac{\partial T}{\partial t} + \rho C_p u \cdot \nabla T + \nabla \cdot q = Q + Q_p + Q_{vd}$$

E. Solution of phase change

When the soil is frozen or melted, it will be accompanied by phase change. When the soil phase changes, the soil absorbs energy, but the temperature does not change. The latent heat in the whole phase transition cannot be Neglect, so how to deal with the phase change process is particularly important.

This time value simulation is to insert a step function for the phase change processing, locate the parameter bar, type the position of the center point in the position text box, and then draw a smooth curve. The phase change material defined is assigned to the model, the phase change material 1 selects ice, the phase change material selects water, and the latent heat of phase change is 333.5 KJ/Kg. Through the above series of processing methods for phase change, the existence of phase transition can be accurately reflected in the simulation.

III. NUMERICAL SIMULATION ANALYSIS OF TEMPERATURE DURING COOLING

According to the basic parameter values and the assignment conditions determined by the indoor test, the calculation model is numerically solved. When the external environment is sealed and there is no air flow in the grating tube, the temperature change of the section in the post-model specimen is shown in Figures 3 and 4 after cooling for 72 hours (3d) and 720 hours(30d).

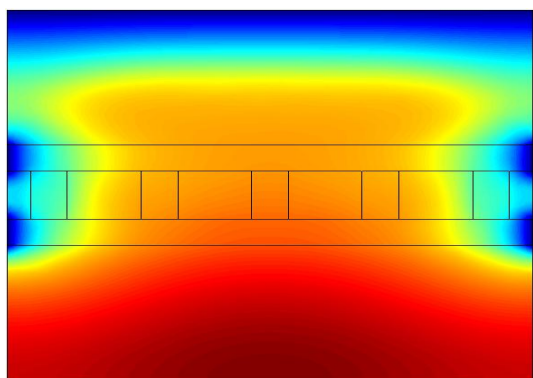


Fig.3 The temperature after 72 hours

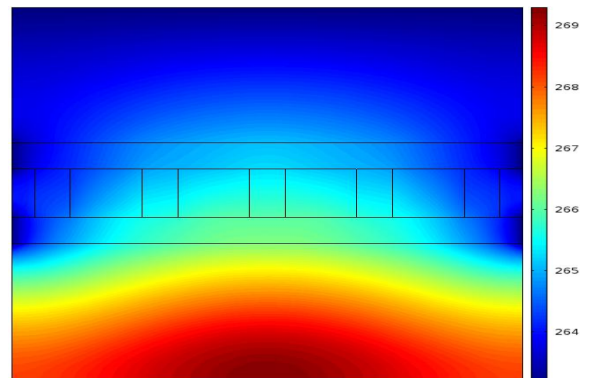


Fig.4 The temperature after 720 hours

It can be seen from the figure that the convective heat transfer is symmetrically distributed on both sides of the grid tube hole. After the external temperature drops to negative temperature, the temperature at the center of the soil drops only to -7.5°C after 15 days without air flow which does not match with the results tested by indoor experiment. After increasing the air flow rate of 0.3m/s, temperature of the whole model drops to below -9°C after 720 hours which is similar to the actual cooling situation. (Figure 5) It also shows that during the cooling process, there must be convective heat transfer between the grid tube and the soil around the tube in the SDG. The temperature change after 720 hours can be determined by the actual situation of air flow in the pipe during the cooling process.

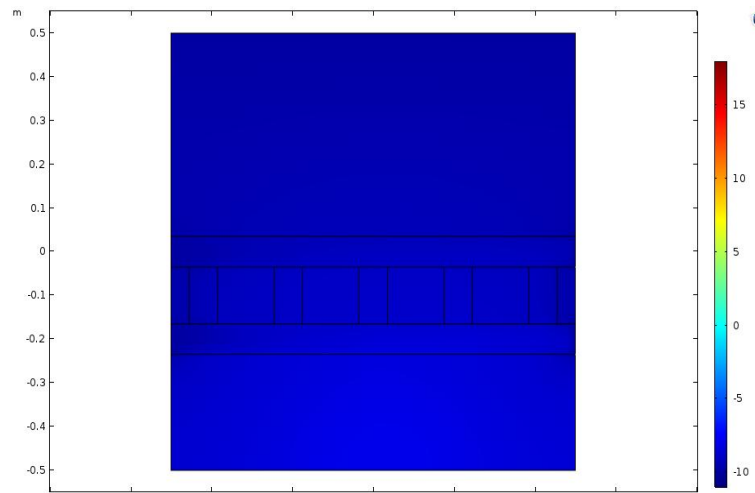


Fig.5 The temperature after 720 hours with flow

After increasing the wind speed of 0.3m/s in the tube, the relationships between temperature and time. The results are as follows:

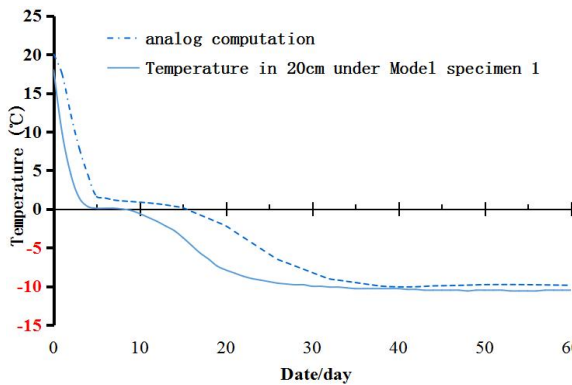


Fig. 6 The 20cm temperature under grille

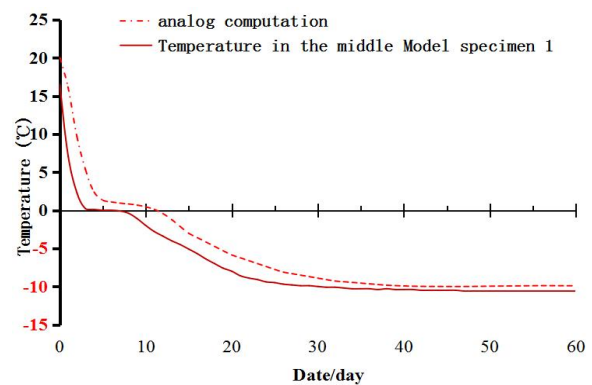


Fig.7 Grid level temperature

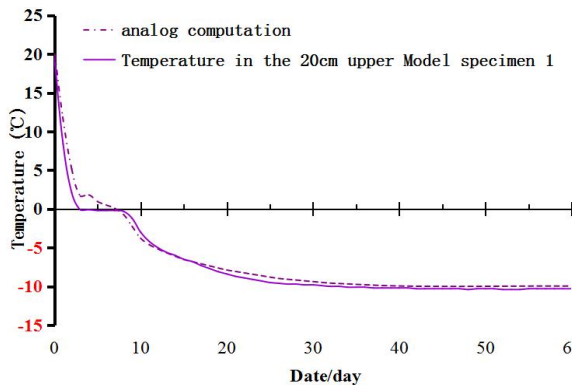


Fig. 8 The 20 cm temperature on the grille

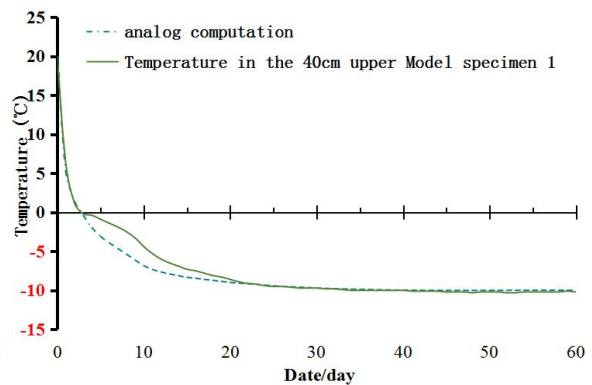


Fig.9 The 40 cm temperature on the grille

The temperature versus time curve of the different measurement points in the finite element calculation results and the indoor model test results. The temperature value of the indoor model test results is basically in the state of zero slope of the curve during the phase transition, and the surface soil is also near zero. Very short phase change process. The temperature change of the 20cm under the grid and the grid layer under the finite element simulation is lagging behind the temperature value measured by the test, and the temperature transition region of the 40cm position on the grid is faster and the phase transition is not obvious.

The reason for the analysis is that the lower part of the grid layer, due to the action of the bottom water source, the capillary water rising channel is still migrating from the “unfrozen zone” to the “freezing zone” before being frozen and cut, and the soil box The thermal insulation layer is not completely adiabatic, and the thermal insulation layer defined by the numerical simulation is completely adiabatic. Therefore, the numerical simulation

of the cooling and phase transformation of the lower part of the grid layer of the model specimen is delayed behind the measured variation. For the 40cm position on the grille, there is a water-repellent layer at the 50cm position on the grille, and 10cm thick soil covering the water-repellent layer. Therefore, when the water freezes, it accumulates on the surface of the water-repellent layer 10cm away from the surface. At the same time, the density and water content of the actual soil model are not absolutely isotropic, so there is a certain difference between the numerical calculation value and the measured value for the temperature change of the surface soil. However, from the comparison of the overall and local temperature values, the fitting degree of temperature with time is still very high.

Figure 10 to Figure 19 show 24 hours (1d), 72 hours (3d), 120 hours (5d), 168 hours (7d), 216 hours (9d), 264 hours (11d), 312 after cooling. Temperature distribution for hours (13d), 408 hours (17d), 480 hours (20d), and 720 hours (30d). It can be seen from the temperature change in the figure that for the soil above the grid, the freezing speed is significantly greater than the freezing speed of the soil at the bottom of the grid by the two-way negative temperature, until the bottom surface and the surface are only 720 hours (30d). By the difference of 2 ° C, the temperature drop effect of the seepage drainage grille is reflected from the temperature change of the model test piece as a whole.

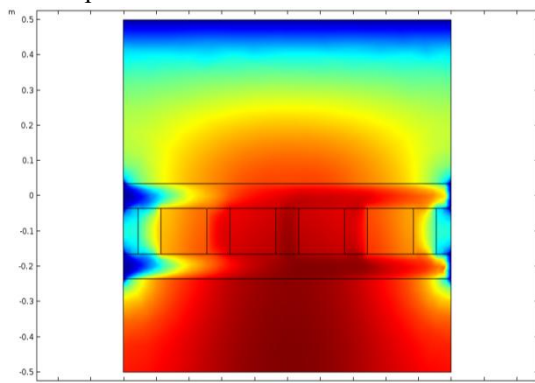


Fig.10 Temperature after 24 hours

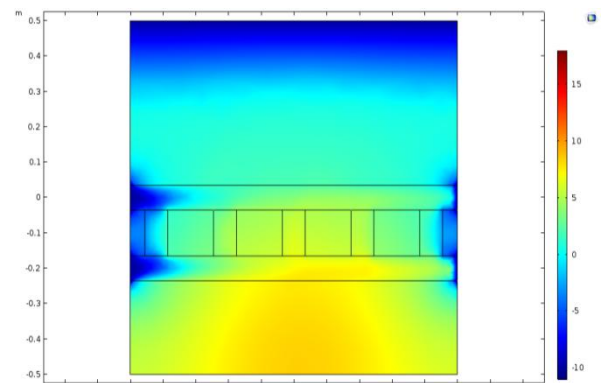


Fig.11 Temperature after 72 hours

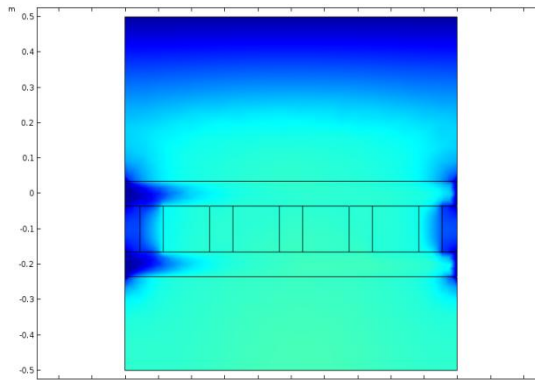


Fig.12 Temperature after 120 hours

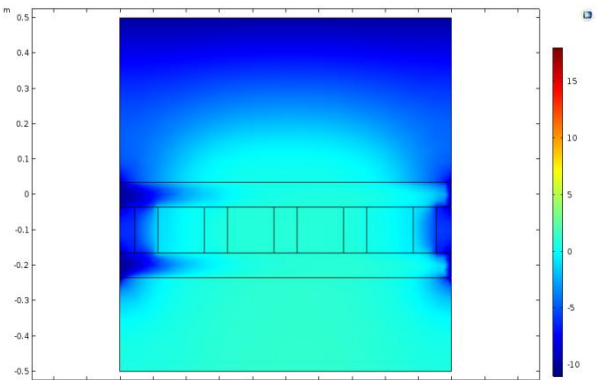


Fig.13 Temperature after 168 hours

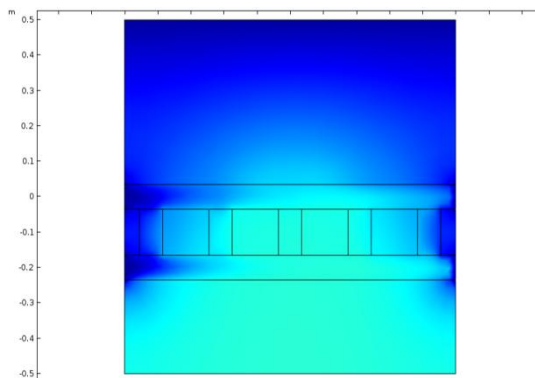


Fig.14 Temperature after 216 hours

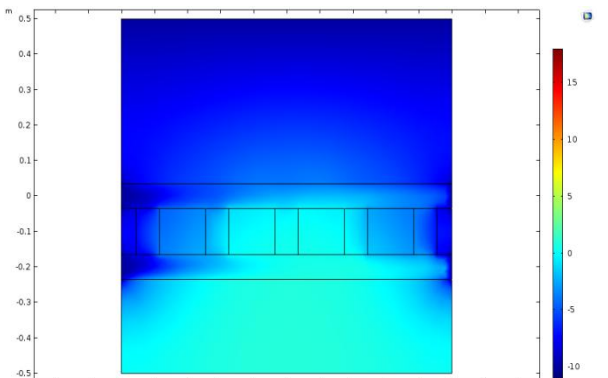


Fig.15 Temperature after 264 hours

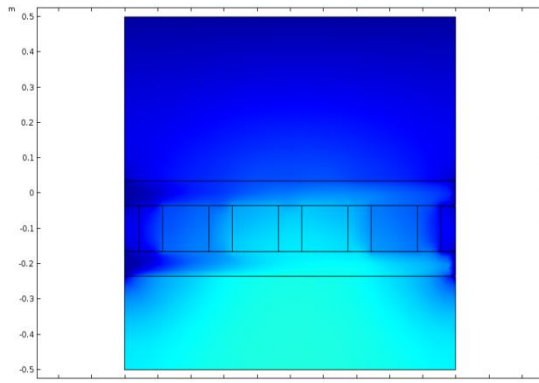


Fig.16 Temperature after 312 hours

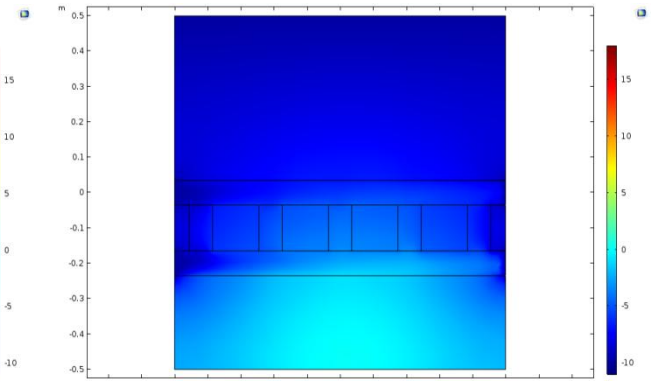


Fig.17 Temperature after 408 hours

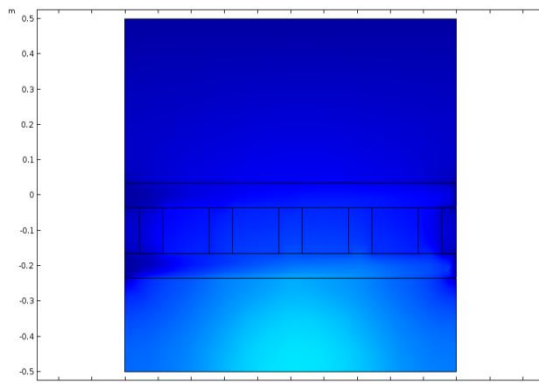


Fig.18 Temperature after 480 hours

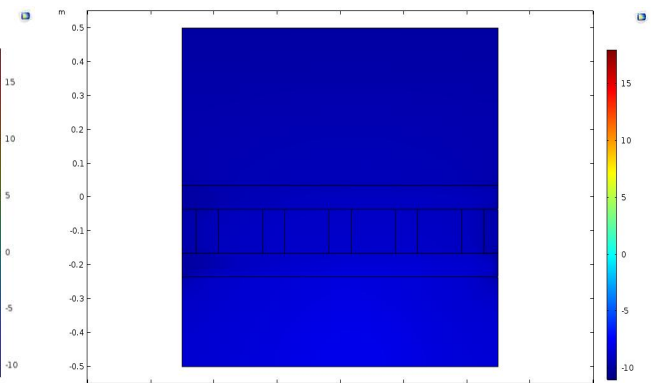


Fig.19 Temperature after 720 hours

IV. NUMERICAL SIMULATION ANALYSIS OF MOISTURE CONTENT DURING HEATING

The overall temperature change of the soil in the model test has been known by numerical simulation, when the external temperature drops to negative. However, it also need numerical simulation analysis as the temperature above zero.

The figure 20 to 23 have illustrated the comparison of moisture content between simulated and measured values when the temperature from below zero to above during the 60 days. And the figure 24 to 31 have shown the change of water content of the model cross section over time after temperature rises 1d, 2d, 3d, 4d, 5d, 10d, 15d and 25d. The figure 30 and 31, however, are different from others owe to the little difference in water content distribution after 360h.

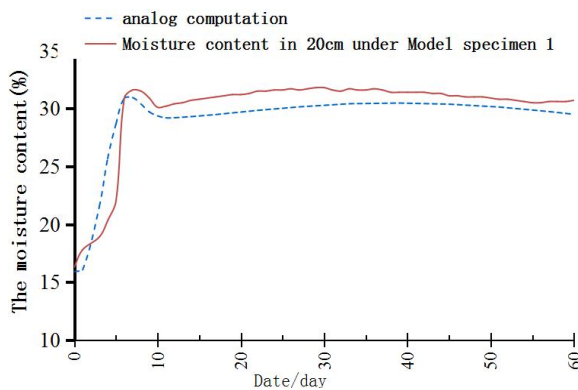


Fig. 20 Moisture content of 20cm under grille

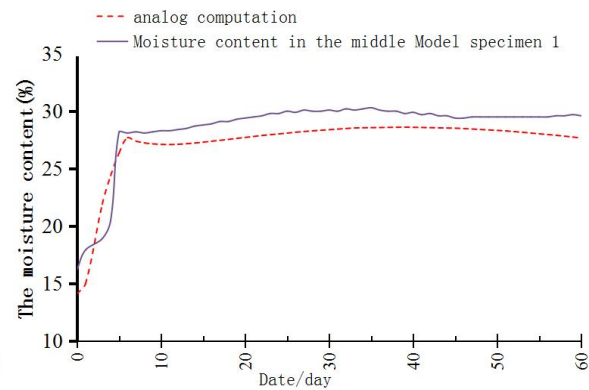


Fig.21 Grid level Moisture content

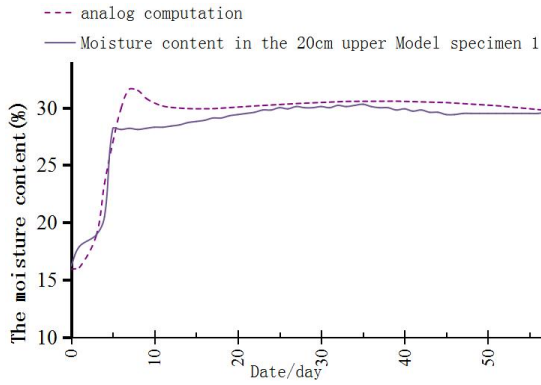


Fig.22 Moisture content of 20cm on the grille

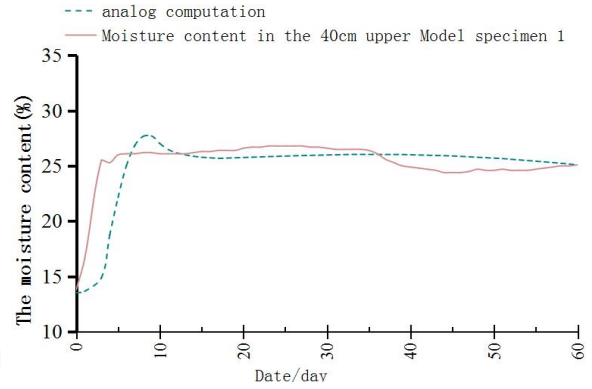


Fig.23 Moisture content of 40cm on the grille

It can be seen from the change of moisture content that the moisture content of the inlet and outlet of the osmotic drainage grid is lower than that of other locations. At the beginning of melting, the change law of moisture content with time is the same as that of temperature. The water rate ladder is the most prominent in 120 hours. After 240h, Moisture content distribution ladder has abated. And after another 120 hours, the water cut ladder distribution almost disappeared. Under the condition of rising capillary water and evaporation of surface water, the water content is uniformly distributed under the influence of drainage action of osmotic drainage grid. The moisture content inside the soil is gradually decreased and evenly distributed along with continuous positive temperature time. We, again, demonstrate the conclusion of previous experiments: The percolation and drainage grid changes the distribution of water field and makes it more uniform.

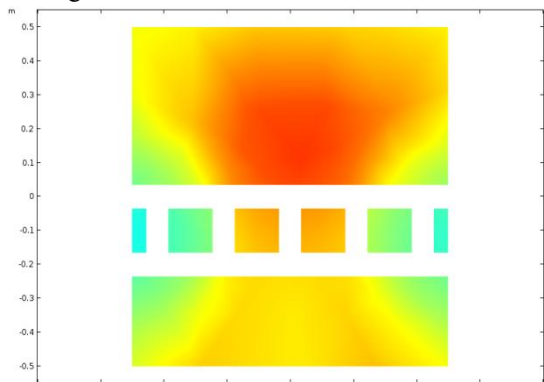


Fig.24 The moisture content after 24 hours

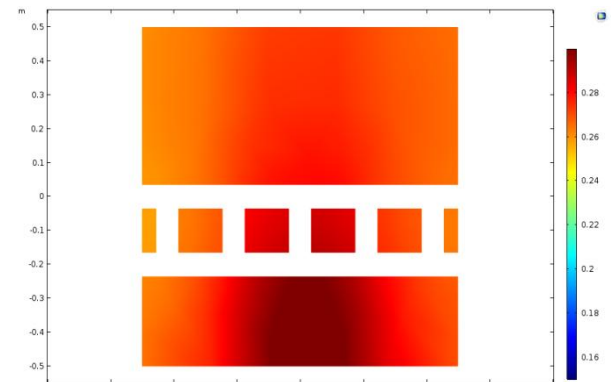


Fig.25 The moisture content after 48 hours

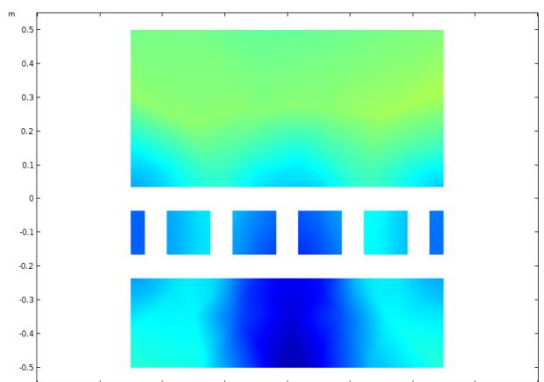


Fig.26 The moisture content after 72 hours

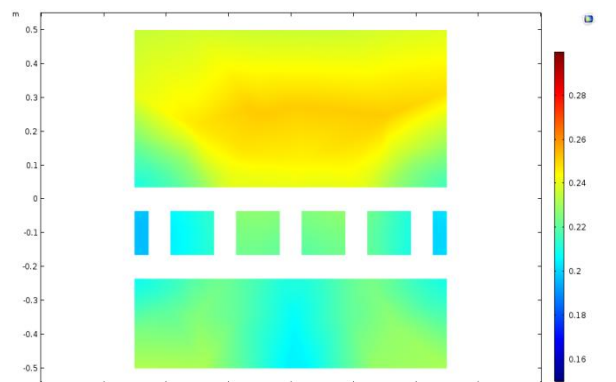


Fig.27 The moisture content after 96 hours

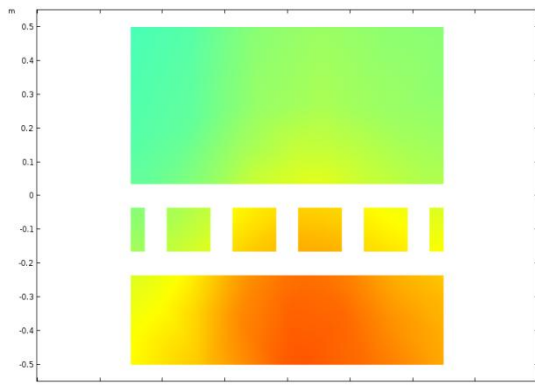


Fig.28 The moisture content after 72 hours

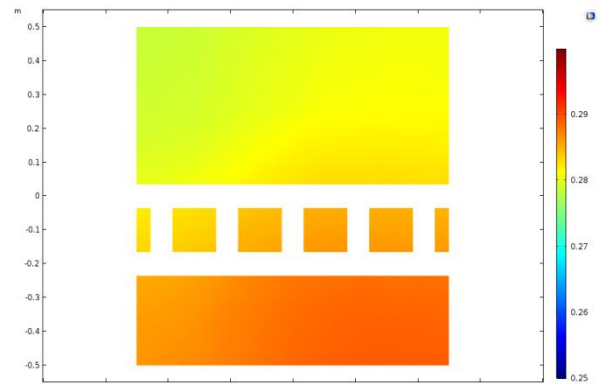


Fig.29 The moisture content after 96 hours

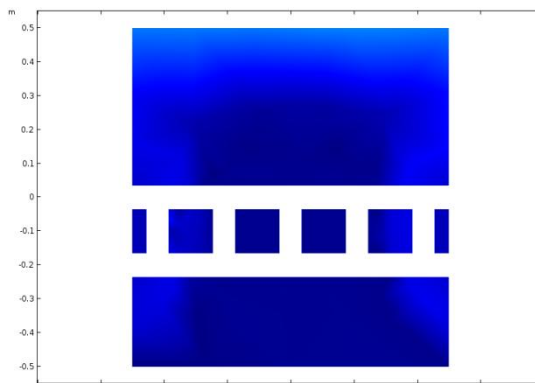


Fig.30 The moisture content after 360 hours

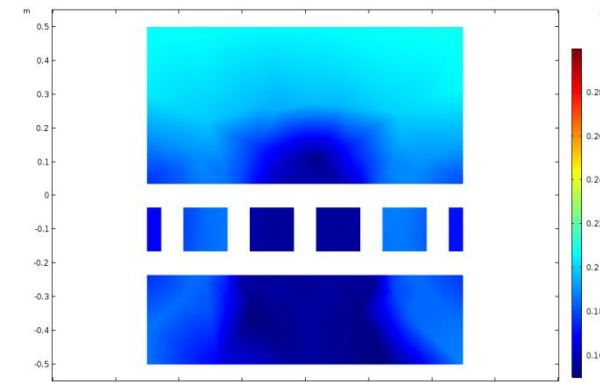


Fig.31 The moisture content after 600 hours

V. MODEL OPTIMIZATION ANALYSIS

By comparing the numerical results of temperature change (cooling Effect) and water content change (drainage Effect) of the indoor model test with those of experimental results, it can be seen that the numerical model and soil water thermal parameters of numerical simulation are accurate and the data curve and the measured data have high fitting degree.

The results of simulation analysis can reflect the change of temperature and moisture content in soil and the distribution of temperature field and water field in the model specimen during Freeze-thaw Cycle.

In this experiment, the grid with gravel layer in model specimens 3 have the best drainage effect, model specimen 1 have the best cooling effect.

therefore, on the basis of maintaining the boundary condition and the model specimen size, the simulation can be conducted by combining with the advantages of these two models, that is to say, using the Grid configuration model of specimen one, and replacing the clay by natural grit.

Fig.32 to 36 for the model specimen one and the temperature comparison of the optimized model, the temperature distribution after cooling 24h (1d), 72h (3d), 120h (5d), 240h (10d), 360h (15d) and Moisture distribution after heating 24h (1d), 72h (3d), 120h (5d), 240h (10d), 360h (15d), 1440h (60d) are selected respectively for Comparison.

The left side of each picture is the original graphic, the right side is optimized graphics, the legend of all the temperature is same, as for the moisture picture, beside Fig 41 and 42, using other legend, the others use the same legend.

Compared with the temperature field in the soil of the optimized seepage and drainage grid (fig.32 to fig.36), the cooling rate of the model is significantly improved after optimization, which indicates that the larger the thermal conductivity of the roadbed filling material with the seepage and drainage grille is, the better cooling effect is.

From the water field comparison (fig.37 to fig.42), since the soil material of the optimized seepage and drainage grid has a larger thermal conductivity, So it is more sensitive to the external temperature. water content reduction is relatively faster from the beginning of the melting of the optimization model. The water content is gradually reduced and the distribution of water field tends to be uniform. therefore, the seepage and drainage grating laid in the material with higher thermal conductivity and porosity have better cooling and drainage effect.

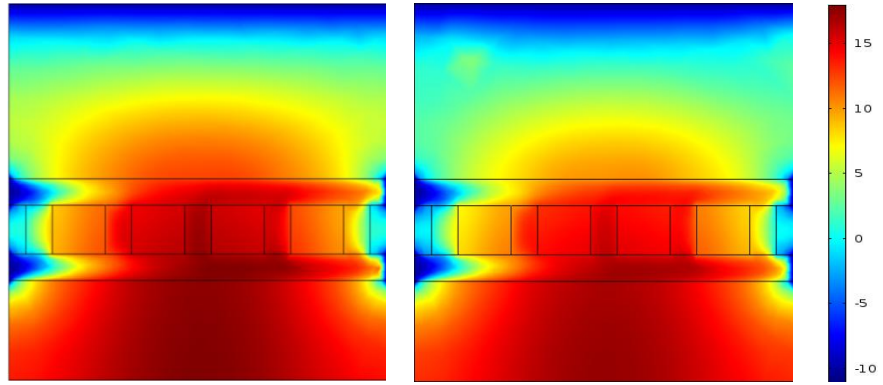


Fig.32 Temperature distribution after 24 hours

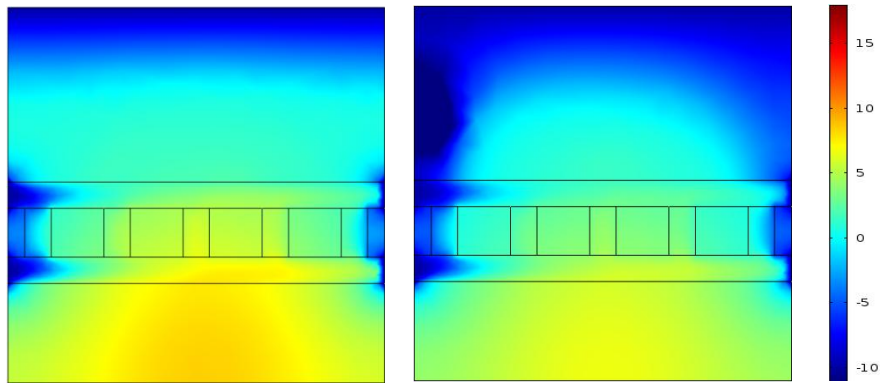


Fig.33 Temperature distribution after 72 hours

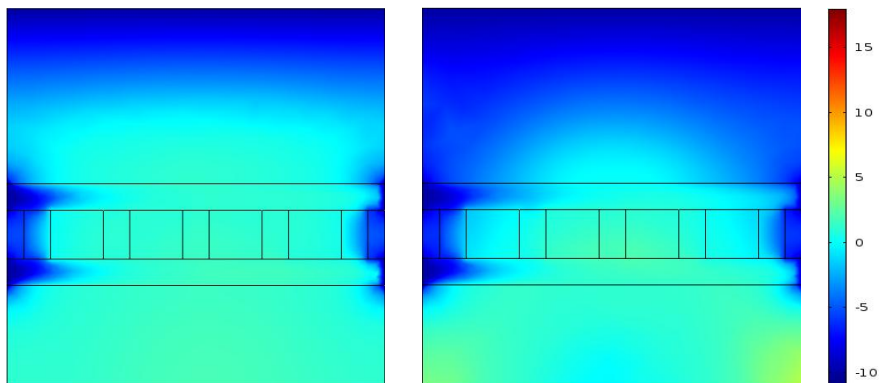


Fig.34 Temperature distribution after 120 hours

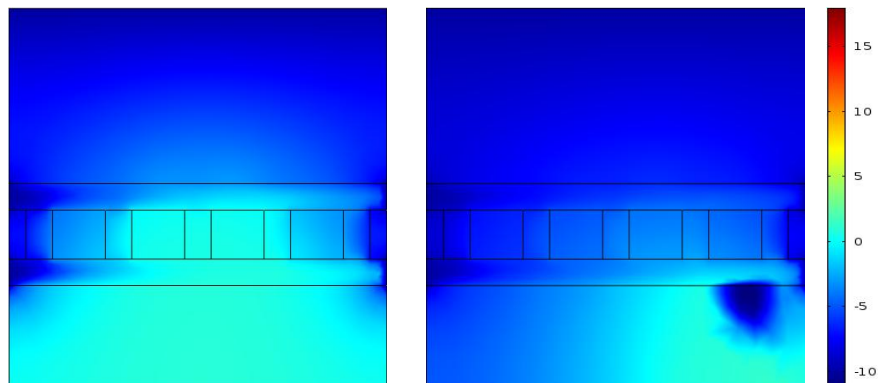


Fig.35 Temperature distribution after 240 hours

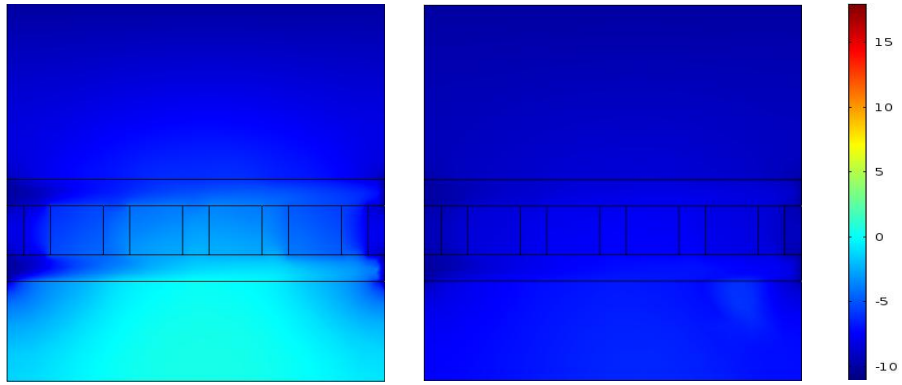


Fig.36 Temperature distribution after 360 hours

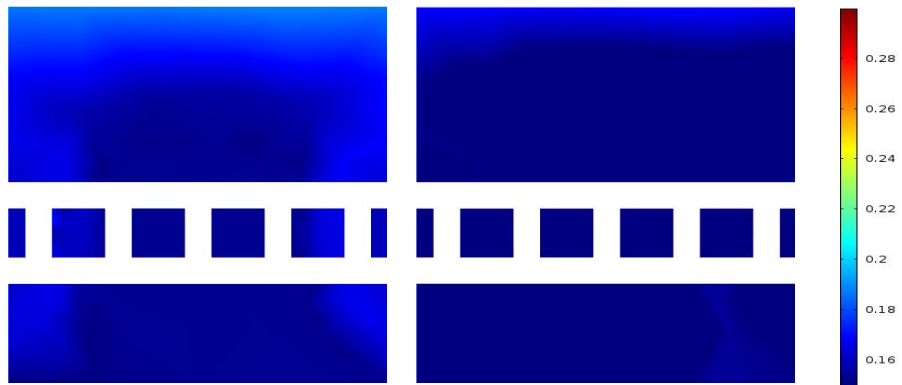


Fig.37 The moisture content after 24 hours

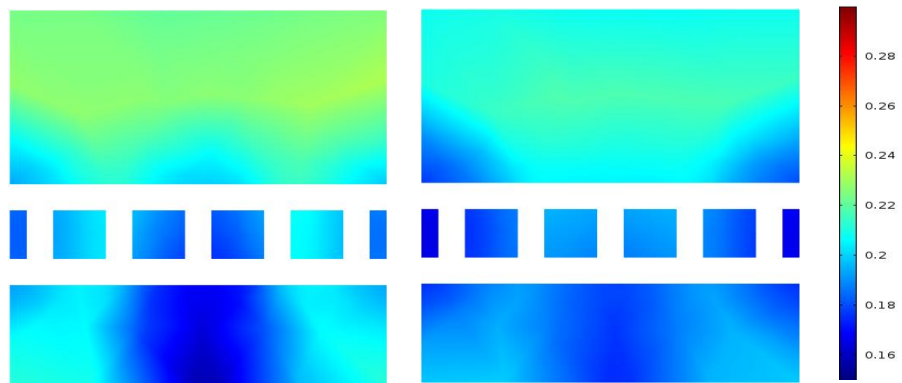


Fig.38 The moisture content after 72 hours

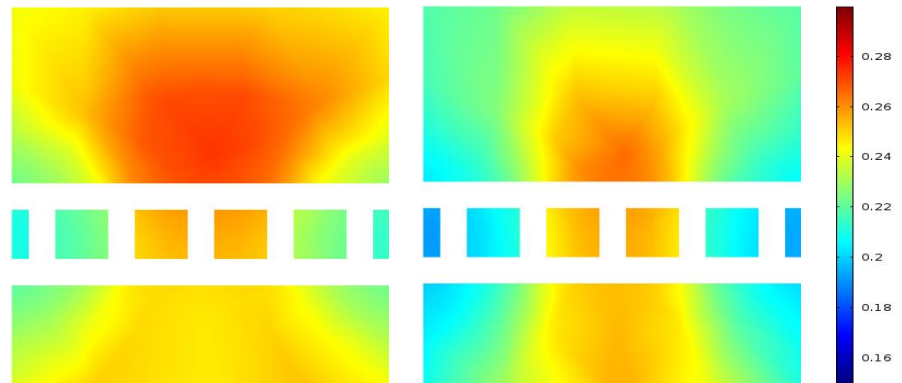


Fig.39 The moisture content after 120 hours

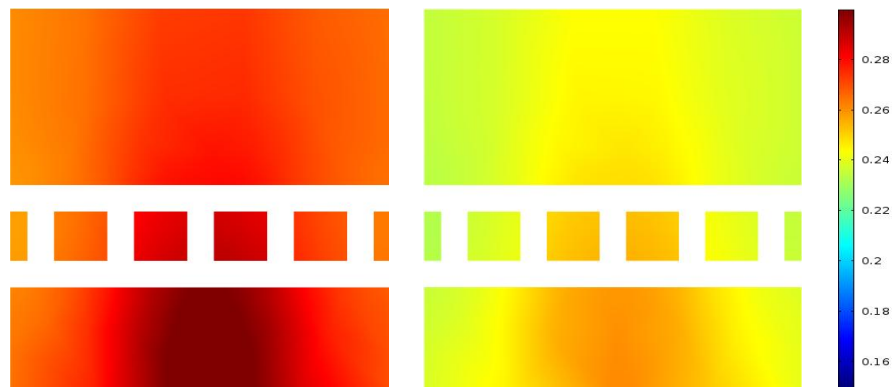


Fig.40 The moisture content after 240 hours

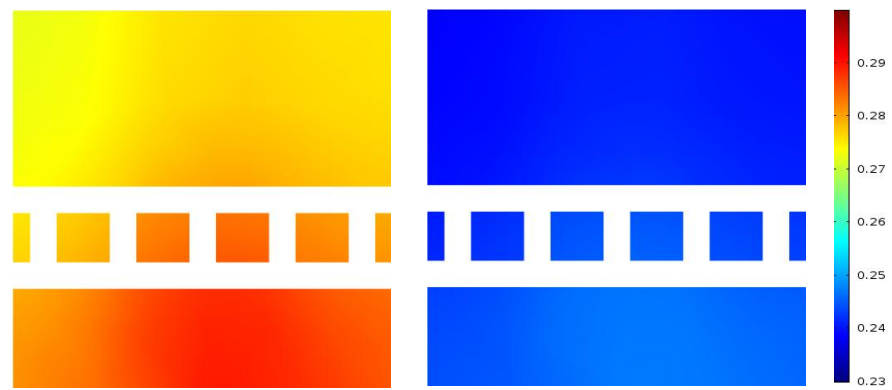


Fig.41 The moisture content after 360 hours

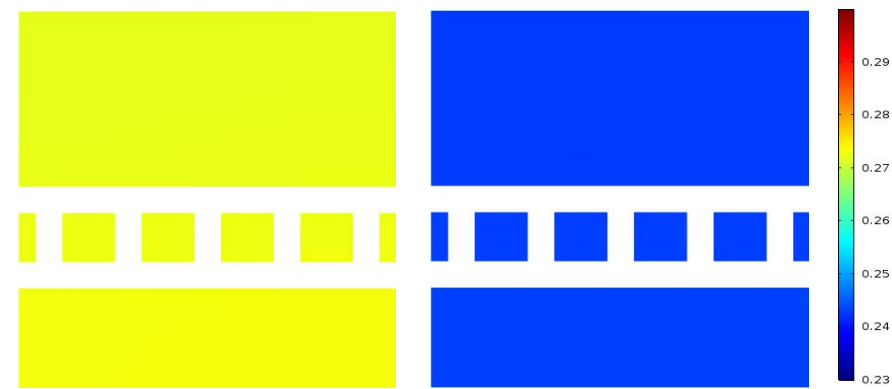


Fig.42 The moisture content after 1440 hours

VI. CONCLUSION

This study proves that the computational model plays a key role in elucidating the hydrothermal mechanism of subgrade soil under the freeze-thaw cycle. By using complex algorithms in the computational platform, it is possible to accurately predict the coupled heat and fluid flows in soil-geosynthetic systems. Validated computer models not only confirm the theoretical framework for soil water transport, but also highlight the complex mass transfer and heat exchange processes facilitated by the SDGS. This heat and humidity management strategy is very important to prevent freezing damage of subgrade structures in cold climates. The computational insights provided in this paper pave the way for informed design decisions and optimization of SDG deployment strategies, thereby enhancing the resilience of transport infrastructure to the harshness of seasonal freeze-thaw cycles.

ACKNOWLEDGEMENTS

1). The research focuses on investigating the freeze-thaw stability mechanism of roadbeds based on the non-thermal equilibrium theory of porous media. (No. LH2023D021).

2). The Scientific Research Project of Hunan Provincial Department of Education-Outstanding Youth. Project under Grant (NO. 23B0737).

REFERENCES

- [1] Yu Q H, Fan K, Qian J, et al. Key issues of highway construction in permafrost regions in China (in Chinese). *Sci Sin Tech*, 2014, 44: 425-432, doi: 10.1360/09 2013-1015.
- [2] About Our Country Frozen Soil Roadbed Processing Method of Course [J]. *Sichuan Building Materials*, 2018,44(4): 156-157.
- [3] Heitman J L, Horton R Ren T, et al. A test of coupled soil heat and water transfer prediction under transient boundary temperatures[J].*Soil Science Society of America Journal*, 2008, 72(5):1197-1207.
- [4] Zhang Z Q, Wu Q B. Freeze-thaw hazard zonation and climate change in Qinghai-Tibet Plateau permafrost. *Nat Hazards*, 2012, 61: 403-423.
- [5] LIU Ge, WAND Shuan-jie, JIN long, DONU Yuan-hong, YUAN Kun[J]. Applicable effect of thermosyphon subgrades in permafrost regions *Journal of Traffic and Transportation Engineering*, 2016, 16(4): 59-66.
- [6] Wang S J, Huang X M, Hou S G. Numerical analyses of pavement deformation and stress in permafrost regions. *J Glaciology Geocryology*, 2006, 28(2): 217-222.
- [7] Wu Q B, Niu F J. Permafrost changes and engineering stability in Qinghai-Xizang Plateau. *Chin Sci Bull*, 2013, 58, doi: 10.1007/s11434-012-5587-z.
- [8] Zheng Qiao Xing. Analysis on Bad Geological Treatment Methods in Highway Permafrost Regions[J]. *Henan Building Materials*, 2018, 4: 7-9.
- [9] MA W, MU Y H, WU Q B, et al. Characteristics and mechanisms of embankment deformation along the Qinghai-Tibet Railway in permafrost regions[J]. *Cold Regions Science and Technology*, 2011, 67(3): 178-186.
- [10] ZHANG M Y, LAI Y M, ZHANG J M, et al. Numerical study on cooling characteristics of two phase closed thermosyphon embankment *Cold Regions Science and Technology in permafrost regions*[J]. 2011, 65(2): 203-210.
- [11] Dong Y B, LAI Y M, XU X T, et al. Using perforated ventilation ducts to enhance the cooling effect of crushed-rock interlayer on embankments in permafrost regions[J]. *Cold Regions Science and Technology*, 2010, 62(1): 76-82 .
- [12] WAND Wei-hua, WU Tony-hua, LI Ren, XIE Chang-wei, ZHU Xiao-fan, An overview of advances on moisture migration of the active layer in permafrost regions of the Qinghai-Tibetan Plateau[J]. *Journal of Northwest Normal University (Natural Science)*, 2017, 53(1): 102-111.